THE JOURNAL OF BIOLOGICAL CHEMISTRY
Vol. 275, No. 11, Issue of March 17, pp. 7910–7917, 2000

Printed in U.S.A.

Cellubrevin Is Present in the Basolateral Endocytic Compartment of Hepatocytes and Follows the Transcytotic Pathway after IgA Internalization*

(Received for publication, February 25, 1999, and in revised form, December 1, 1999)

Maria Calvo‡§, Albert Pol‡§, Albert Lu‡, David Ortega‡, Mònica Pons‡, Joan Blasi¶, and Carlos Enrich‡‖

From the ‡Departament de Biologia Cel.lular, Institut de Investigacions Biomèdiques August Pi i Sunyer, Facultat de Medicina and the ¶Departament de Biologia Cel.lular, Facultat d'Odontologia, Universitat de Barcelona, 08036 Barcelona, Spain

The endocytic compartment of polarized cells is organized in basolateral and apical endosomes plus those endocytic structures specialized in recycling and transcytosis, which are still poorly characterized. The complexity of the various populations of endosomes has been demonstrated by the exquisite repertoire of endogenous proteins. In this study we examined the distribution of cellubrevin in the endocytic compartment of hepatocytes, since its intracellular location and function in polarized cells are largely unknown. Highly purified rat liver endosomes were isolated from estradiol-treated rats, and the early/sorting endosomal fraction was further subfractionated in a multistep sucrose density gradient, and studied. Analysis of dissected endosomal fractions showed that cellubrevin was located in early/sorting endosomes, with Rab4, annexins II and VI, and transferrin receptor, but in a specific subpopulation of these early endosomes with the same density range as pIgA and Raf-1. Interestingly, only in those isolated endosomal fractions, endosomes enriched in transcytotic structures (of livers loaded with IgA), the polymeric immunoglobulin receptor specifically co-immunoprecipitated with cellubrevin. In addition, confocal and immuno-electron microscopy identification of cellubrevin in tubular structures underneath the sinusoidal plasma membrane together with the re-organization of cellubrevin, in the endocytic compartment, after the IgA loading, strongly suggest the involvement of cellubrevin in the transcytosis of pIgA.

Receptor-mediated endocytosis is a process in which eukaryotic cells selectively internalize macromolecules and a large variety of extracellular solutes. In general, the main features of this pathway are relatively well understood and involve the internalization of receptor/ligand complexes via clathrin-coated pits and vesicles that rapidly lose their coat to fuse with the early/sorting endocytic compartment. Whereas receptors are sorted and diverted into a complex tubular network of membranes, and recycle back to the plasma membrane, ligands are targeted into the late endosomes and eventually to the lysosomal compartment for degradation. Although this is still considered the main route, different ports of entry have now been described, for example by non-clathrin-coated pits and/or by caveolae (1). Indeed, the endocytic destination for these different ports of entry could also differ, as could the connections between intracellular pathways along the endocytic stations, which are multiple and complex. Thus, whether endosomes undergo maturation (2) or whether endocytic carrier vesicles are transported through pre-existing (3) early and late endocytic compartments is still a matter of controversy. Besides, the possibility that, in some cells, early and late endosomes are part of an extensive tubular endocytic network has recently been shown (4).

In polarized epithelial cells, surface polarity is generated and maintained by the membrane trafficking along the exocytic and endocytic pathways. For this reason, it is crucial to understand the molecular mechanism(s) as well as the endosomal constituents which contribute to these processes.

Cellubrevin is a ubiquitous intracellular integral membrane protein involved in the constitutive recycling pathway (5, 6). It belongs to the v-SNARE[1] family (synaptobrevin/VAMP-related protein) and, like synaptobrevin II (VAMP-2), it is proteolysed by tetanus toxin light chain. Recently, the localization of different SNAREs in MDCK cells and in CaCo-2 cells has been defined (7, 8). Galli *et al.* (8) showed that cellubrevin was present in both the lateral and the apical membrane domains of CaCo-2 cells. However, its precise function in polarized cells remains unknown.

In the hepatocyte, it is generally assumed that there is a default biosynthetic transport of membrane proteins to the basal surface (sinusoidal plasma membrane). From there on and through the endocytic compartment, there is a specialized transcellular transport to the bile canalicular plasma membrane (apical domain), where transcytosis is accomplished (*e.g.* transcytosis of pIgA). Although this is assumed to be the main route, evidence for direct targeting into the apical (bile canalicular) plasma membrane has been reported (9–11). Less known is the route for the incorporation of membrane proteins into the lateral plasma membrane, *e.g.* connexins, which assemble in a gap junction (12), or desmosomal glycoproteins.

* This work was funded by Ministry of Education Grant PM96-0083 (to C. E.). The costs of publication of this article were defrayed in part by the payment of page charges. This article must therefore be hereby marked "*advertisement*" in accordance with 18 U.S.C. Section 1734 solely to indicate this fact.

§ These authors made equal contribution to this work.

‖ To whom correspondence should be addressed: Dept. de Biologia Cel.lular, Facultat de Medicina, Universitat de Barcelona, Casanova 143, 08036 Barcelona, Spain. Fax: 34-93-4021907; E-mail: enrich@medicina.ub.es.

[1] The abbreviations used are: v-SNARE, vesicle-associated SNAP receptor; pIgA, polymeric IgA; CURL, early-sorting endosomes (compartment of uncoupling receptors and ligands); MDCK, Madin-Darby canine kidney; MVB, late endosomes (multivesicular bodies); NEM, *N*-ethylmaleimide; NSF, NEM-sensitive factor; pIgR, polymeric immunoglobulin receptor; RRC, recycling and transcytotic endosomes (receptor-recycling compartment); SNAP, soluble NSF attachment protein; t-SNARE, target-associated SNAP receptor; VAMP, vesicle-associated membrane protein; FITC, fluorescein isothiocyanate; PBS, phosphate-buffered saline; LDL, low density lipoprotein; BSA, bovine serum albumin.

Two different intracellular regions actively involved in the sorting and processing of endocytosed ligands and receptors have been depicted in the hepatic cell: 1) the subapical endocytic compartment (13, 14) involved in the deep recycling of receptors, such as the ASGP-R (15), in the late stages of transcytosis of pIgA (16) and defined by its enrichment of annexin VI (17). Topologically, is located around the bile canaliculus and is close to the Golgi-lysosomal region of the cell. 2) Less characterized are the basolateral early/sorting endosomes at the subsinusoidal region of hepatocyte, presumably involved in the rapid (constitutive) recycling of receptors back to the sinusoidal plasma membrane, in the early sorting of molecules for transcytosis and, as shown recently, in the activation of signal transduction (18).

In this study we demonstrated that cellubrevin is specifically located in these early/sorting subsinusoidal endocytic structures. It shows an almost restricted location underneath the sinusoidal plasma membrane of hepatocytes, but after exogenous pIgA uptake it "moves" to the subapical domain, along the transcytotic pathway. Since no change in the cellubrevin-staining pattern was observed, in livers loaded with ligands that enter by receptor-mediated endocytosis (*e.g.* LDL) or by fluid phase markers (e.g dextran-FITC) and that follow the degradation pathway, we conclude that cellubrevin may be involved in transcytosis of IgA through the endocytic compartment.

EXPERIMENTAL PROCEDURES

Animals and Reagents—Male Harlan Sprague-Dawley rats weighing 200–250 g were maintained under a controlled lighting schedule with 12-h dark period. All animals received humane care in compliance with institutional guidelines. Food and water were available *ad libitum*.

pIgA was from Nordic Immunological Laboratories (Tilburg, The Netherlands); dextran-FITC (M_r 70,000) was from Molecular Probes (Leiden, The Netherlands). Human LDL ($1.025 < d < 1.050$ g/ml) was isolated from normolipidemic adult humans (19).

Antibodies—The rabbit polyclonal affinity-purified antibody to membrane-bound annexin VI (17) was provided by Dr. S. Jäckle (University of Hamburg), and the rabbit affinity-purified anti-cellubrevin (20) was prepared in our laboratory. Mouse anti-transferrin receptor and anti-pIgR (SC-166) monoclonal antibodies were kindly provided by Dr. K. E. Mostov (University of California, San Francisco, CA). Mouse monoclonal antibodies to anti-annexin II (A14020) and anti-Raf-1 (R-19120) were from Transduction Laboratories (Lexington, KY). Rabbit polyclonal affinity-purified anti-Rab4 (sc-312) was from Santa Cruz Biotechnology (Santa Cruz, CA). A rabbit anti-human apoB100 polyclonal antibody was kindly donated by Dr. Ulrike Beisiegel (University of Hamburg). Finally, a monoclonal anti-human IgA (α-chain-specific) (clone GA-112) was from Sigma (Madrid, Spain). Fluorescently conjugated (FITC and Cy 3) antibodies were from Jackson ImmunoResearch (West Grove, PA).

Isolation of Endosomes and Plasma Membrane from Rat Liver—After 3 days of 17-α-ethinyl estradiol treatment to induce the expression of the low density lipoprotein receptors (21), rats were anesthetized with isofluorane, and human LDL (5 mg of protein) was injected into the femoral vein. 20 min later, livers were removed and homogenized in 0.25 M sucrose with protease inhibitors. The method used for the isolation of the endosomal fractions from rat liver is described elsewhere (22, 23). Three distinct endosomal fractions were obtained after centrifugation of a crude endosome fraction in a sucrose gradient: MVB at 8.24%/19.3%, CURL at 19.3%/28.81%, and RRC at 28.81%/36.37% (w/v) interfaces. Each fraction was collected, and ice-cold water was added to render the fractions isotonic. The isotonic fractions were pelleted, resuspended in 0.9% NaCl, and stored at −80 °C.

In some experiments, the interface corresponding to CURL or to RRC were mixed with heavy sucrose (2.5 M) and loaded at the bottom of a discontinuous sucrose gradient with 19%, 21%, 23%, 25%, 27%, and 29% sucrose (w/v) for CURL or 29%, 31%, 33%, 35%, 37%, and 39% for RRC, and the tubes were centrifuged at 28,000 rpm for 2 h 50 min, in a Beckman SW28 rotor. Following centrifugation, the interfaces were unloaded, pelleted, resuspended in 0.9% NaCl, and stored at −80 °C. The same procedure was also performed in those experiments where IgA was injected into the portal vein.

A plasma membrane fraction derived from the lateral and canalicular domains of the hepatocyte was isolated essentially according to the method described by Neville (24).

Gel Electrophoresis, Immunoblots, Immunoprecipitation, and Densitometry—SDS-PAGE of proteins was performed in 10% or 12% polyacrylamide, as described by Laemmli (25). For Western blotting, polypeptides (3–5 μg of protein/channel) were transferred electrophoretically at 60 V for 60–90 min at 4 °C (depending on the proteins to be identified) to Immobilon-P transfer membranes (Millipore), and antigens were identified using specific antibodies diluted in Tris-buffered saline containing 0.5% powdered skimmed milk, and finally the reaction product was detected using the ECL system (Amersham Pharmacia Biotech). Image analysis of Western blots and band quantification were performed with a Bio-Image system (Millipore).

For cellubrevin immunoprecipitation, 50 μg of protein of the endosomal fractions RRC and CURL, from control and from IgA-injected rats, were solubilized with 1% Triton X-100, 10 mM Hepes, pH 7.4, 140 mM KCl, 10 mM EDTA on ice, containing the following proteinase inhibitors: 50 mM NaF, 0.1 mM sodium vanadate, 1 mM phenylmethylsulfonyl fluoride, and 10 μg/ml leupeptin. After removal of the insoluble material in a microcentrifuge, the soluble fractions were incubated with rabbit anti-cellubrevin antibody or with normal rabbit serum (control) overnight at 4 °C. Protein immunocomplexes were then incubated with Protein A-Sepharose (Pierce) for 1 h at 4 °C, collected by centrifugation, and washed three times with the same buffer used for solubilization except that 0.1% Triton X-100 was used.

For the pIgR immunoprecipitation, the mouse monoclonal anti-pIgR antibody (SC-166) was used according the procedure described by Luton *et al.* (26); briefly, liver endosomal fractions (50 μg of protein), with or without IgA, were solubilized in a freshly buffer of 1% Nonidet P-40, 125 mM NaCl, 20 mM HEPES (pH 7.4), 10 mM NaF, 2 mM sodium vanadate, and protease inhibitor mixture. After washing, immunoprecipitated proteins were resolved by SDS-PAGE, and the presence of coimmunoprecipitated pIgR or cellubrevin analyzed by Western blotting. A nonrelated monoclonal antibody was used as control.

The protein content of the samples was measured by the method of Bradford (27) using bovine serum albumin as standard.

Immunofluorescence Studies in Liver and in Isolated Primary Cultured Hepatocytes: Uptake of pIgA, LDL, Transferrin-FITC, and Dextran-FITC—pIgA (100 μg), LDL (5 mg), or dextran-FITC (5 mg) (M_r 70,000) or 0.9% NaCl for control animals, were injected into the portal vein (except for LDL, which was injected into the femoral vein) of Harlan Sprague-Dawley (200–250 g) rats anesthetized with isofluorane, and 2.5 or 20 min later livers were perfused with 2% paraformaldehyde-PBS (50 ml). Small pieces of liver were post-fixed for 2 h in the same fixative, then washed in PBS and cryoprotected by sucrose embedding, and finally frozen on dry ice. Cryostat sections (6–8 μm) were obtained, air-dried, and hydrated in PBS before immunostaining (15). Confocal microscopy (Leica TCS NT) was used to collect the images, equipped with a 63× Leitz Plan-Apo objective (numeric aperture 1.4). Images represent approximately 1.0-μm optical sections. Adobe Photoshop software (Adobe Systems, San Jose, CA) was used for image processing.

Finally, in some experiments, hepatocytes in primary culture were prepared from Harlan Sprague-Dawley rats by liver perfusion using collagenase type IV (28) (30 μg/ml Hanks' medium) (Sigma). Isolated hepatocytes were allowed to attach overnight at 37 °C in a CO_2 incubator before fixation.

In hepatocytes, transferrin-FITC (20 μg/ml) in 0.5% BSA/Hepes-buffered serum-free medium was internalized over 60 min. After washes, cells were fixed in PLP (4% paraformaldehyde in 40 mM sodium phosphate, 75 mM lysine buffer (pH 7.4) containing 9.1 mM sodium periodate) fixative and permeabilized with 0.1% saponin in 0.5% BSA/PBS, 20 mM glycine for 10 min. Cells were subsequently processed for indirect immunofluorescence with anti-cellubrevin antibody and a goat anti-rabbit IgG F(ab)′$_2$-conjugated-Cy 3 secondary antibody. Finally, cells on coverslips were mounted on glass slides with Mowiol and examined under a confocal microscope.

Immunoelectron Microscopy—For electron microscopy, rat livers were perfused *in situ* with 50 ml of PBS containing 2 mM $CaCl_2$ and 2 mM $MgCl_2$ and then with 100 ml of 2% paraformaldehyde, 0.1% glutaraldehyde in 0.1 M phosphate buffer, pH 7.2, containing 3% polyvinylpyrrolidone (15). Liver pieces were placed in cold fixative, further dissected, and left in fixative overnight at 4 °C. The tissue was then washed in PBS and incubated in 0.5 M NH_4Cl in PBS for 60 min. at 4 °C. After washing in PBS, the tissue was dehydrated with increasing concentrations of ethanol in distilled water (30 min/change) on ice up to 75% ethanol, transferred to 95% ethanol and then to absolute ethanol, both changes at −20 °C for 2 h each. Tissue samples were then infil-

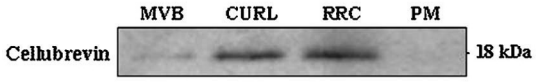

FIG. 1. **Distribution of cellubrevin in rat liver endosomes.** Representative Western blot of cellubrevin distribution in isolated rat liver endosomes and plasma membrane (4 μg/lane). CURL (45 ± 5%) and RRC (40 ± 8%) are the endosomal fractions enriched in cellubrevin (n = 7). *PM*, hepatocyte plasma membrane fraction.

trated with Lowicryl K4M:ethanol (1:2 and then 2:1 at −20 °C for 1 h each) and then with daily changes of undiluted Lowicryl for 1 week at −20 °C. For polymerization, each piece of liver was transferred to a gelatin capsule containing Lowicryl and left under UV (360 nm) overnight at −35 °C and then for additional 48 h at room temperature. Ultrathin sections were cut using a Reichert Ultracut E microtome and collected on Formvar-coated gold grids. For cellubrevin localization, grids were incubated for 1 h at room temperature with primary antibodies (1:10) in PBS containing 1% BSA. After washing, the grids were incubated for 1 h at room temperature with protein A conjugated to colloidal gold particles in PBS containing 1% BSA, 0.075% Triton X-100, 0.075% Tween 20. After several washes, sections were stained with saturated ethanolic uranyl acetate, counterstained with lead citrate, and examined in a Hitachi HT-600 electron microscope. As control for immunostaining, sections were incubated with the second antibodies (protein A-gold) only; the labeling was specific as no signal was obtained (data not shown).

RESULTS

Cellubrevin is a ubiquitous integral membrane protein, abundantly expressed in the liver but with a completely unknown intracellular location and function. By using an affinity-purified polyclonal antibody to cellubrevin (developed and characterized in our laboratory (Ref. 20)), we studied the intracellular distribution of this v-SNARE protein in rat liver and in isolated endosomes.

Highly purified endosomes from estradiol-treated rats were used to find out the distribution of cellubrevin in the hepatic endocytic compartment. The high level of purity of the three endosomal fractions, isolated from rat liver by the method developed by Havel and co-workers, is well documented (22, 23, 29–33). Recently, we have also carried out a detailed comprehensive biochemical characterization of these endosomal fractions (18, 34–36).

Cellubrevin Distribution in Isolated Rat Liver Endosomes—Fig. 1 shows the distribution of cellubrevin by Western blotting in the endosome and plasma membrane fractions isolated from rat liver. Cellubrevin was specifically enriched in two of the endosomal fractions (CURL, 45% and RRC, 40%). The late endosomal fraction (MVB) contained only 15% of the total cellubrevin. Cellubrevin was also detected in a Golgi-isolated fraction (10 -20%, compared with the amount of TGN38; data not shown) but was not detected in a plasma membrane fraction isolated from rat liver (this fraction was mainly from the canalicular/lateral plasma membrane domains). CURL has been characterized as the early/sorting compartment, whereas the RRC is a more complex fraction that includes recycling (22, 23) and transcytotic endosomes (37) but also contains caveolin (38). Electron microscopy of isolated fractions showed the differential morphology between isolated endosomes; whereas MVB is always a very homogeneous fraction, CURL and RRC showed a certain degree of heterogeneity, most probably reflecting the presence of various subpopulations of "early" and "recycling" endosomes.

In order to dissect and further characterize the early endocytic structures, we attempted to separate them in an additional subfractionation step. Isolated CURLs were loaded in an additional continuous sucrose density gradient, and fractions were separated by flotation at 28,000 rpm for 2 h and 50 min (see "Experimental Procedures" for details). Samples unloaded from different densities of the gradient were analyzed by Western blotting. The amount and the distribution of annexin VI, transferrin receptor, Rab4, and annexin II were very similar along the 19–29% (w/v) sucrose density gradient (Fig. 2). Interestingly, cellubrevin, pIgA, and Raf-1 showed a more restricted distribution, with a peak in the middle of the sucrose gradient (25% sucrose).

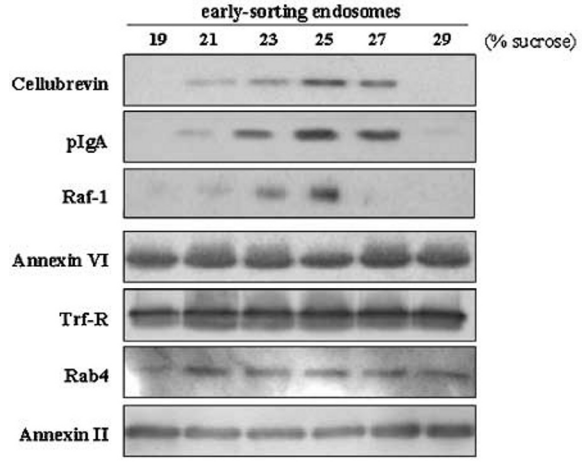

FIG. 2. **Biochemical dissection of CURL.** Isolated early sorting endosomes (CURL) were loaded at the bottom of a multistep sucrose gradient (from 17% to 31% w/v) and centrifuged for 2 h and 50 min at 20,800 rpm, in a SW28 rotor. Samples from this gradient (2 ml) were pelleted, resuspended in 0.9% NaCl, TCA-precipitated, electrophoresed (4 μg/lane), and transferred to Immobilon-P membranes. Western blotting was used to analyze the distribution of proteins along the gradient.

Intracellular Location of Cellubrevin in Rat Liver: Confocal and Electron Microscopy—The distribution of cellubrevin was studied and compared with annexin VI as an endosomal marker for the apical endosomes (17). Examination of frozen sections of rat liver treated with the affinity-purified anti-annexin VI antibody showed that fluorescence was concentrated predominantly in the canalicular (apical) region of hepatocytes (Fig. 3*b*). The staining with anti-cellubrevin affinity-purified antibody shows the labeling in the subsinusoidal (basal) region of hepatocytes (Fig. 3*a*) (double labeling was not attempted because both antibodies were polyclonal). Controls using antibodies to antigens located at the plasma membrane of endothelial cells (RECA-1) clearly showed labeling with anti-cellubrevin in the hepatocyte (data not shown).

In some experiments, the intracellular location of cellubrevin was also examined in primary cultured hepatocytes. Cellubrevin showed a punctate, vesicular, staining underneath the plasma membrane around single cells or, in couplets, it was also observed in the pericanalicular (Golgi-lysosomal) region (Fig. 3*c*). In these experiments, transferrin-FITC was internalized for 60 min, then cells were fixed and immunolabeled with anti-cellubrevin antibody; Fig. 3*d* shows that cellubrevin did not co-localize with the recycling transferrin compartment, in the perinuclear region of hepatocytes.

Finally, to examine in more detail the type of structures labeled by the anti-cellubrevin antibody, immuno-electron microscopy was performed on Lowicryl sections. Fig. 4 shows representative areas in which intracellular subsinusoidal structures were labeled with anti-cellubrevin antibody (protein A and 10 nm gold used as a secondary antibody). Tubules, but also vesicles and tubulovesicular endocytic structures close to the sinusoidal plasma membrane, can be observed with scattered gold labeling on the cytoplasmic face. A few small vesicles were also labeled with anti-cellubrevin in the pericanalicular region of the hepatocyte (subapical endocytic compartment), where most of the endocytic structures were larger and with vesiculotubular morphology (positive for annexin VI; see

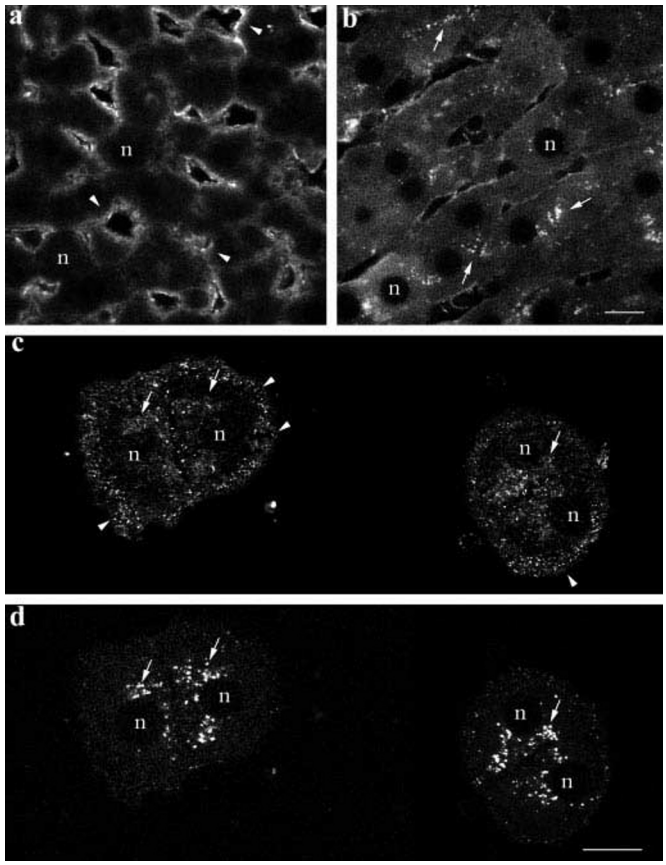

FIG. 3. **Immunocytochemical distribution of cellubrevin in rat liver and in isolated hepatocytes.** Frozen sections from rat liver (6–8 μm) were used to study the localization of cellubrevin (*a*) and compared with annexin VI (*b*). Sections were incubated with respective primary antibodies, followed by anti-rabbit FITC-conjugated secondary antibodies. Cellubrevin labeling is concentrated in the subsinusoidal region of hepatocytes (*arrowheads*). On the other hand, annexin VI is mostly in the pericanalicular (subapical) regions of hepatic cells (*arrows*). Isolated primary cultured hepatocytes (*c* and *d*) were also used to examine the intracellular location of cellubrevin (*c*) and to compare with the location of the recycling endocytic compartment (*d*). Transferrin-FITC was internalized for 60 min, and cells were fixed and immunolabeled with anti-cellubrevin antibody. In couplets of hepatocytes, cellubrevin showed a punctate pattern underneath the plasma membrane but also in the pericanalicular region (Golgi-lysosomal region). After 60 min (pulse) of transferrin-FITC internalization (*d*), pairs of *arrows* in *c* and *d* point the little co-localization of transferrin-FITC and cellubrevin in the perinuclear recycling endosomes. *Bar* is 10 μm.

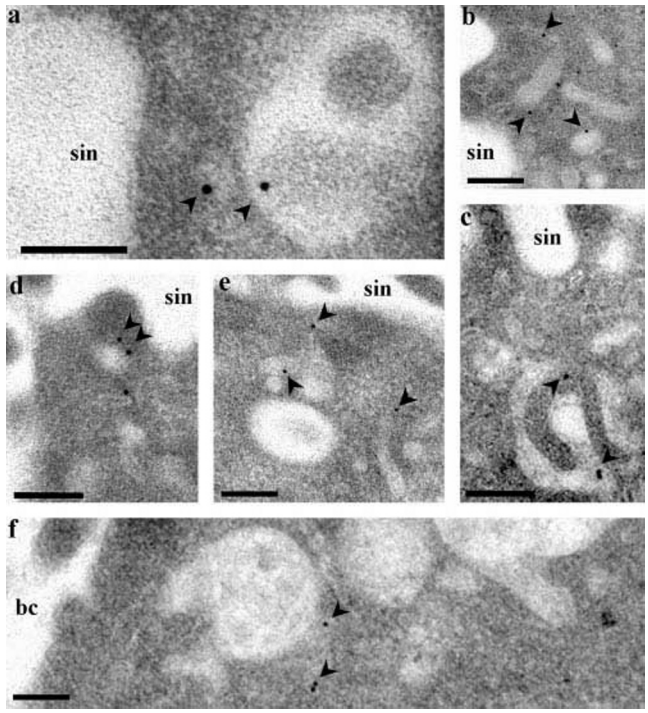

FIG. 4. **Localization of cellubrevin in rat liver: immunoelectron microscopy.** Ultrathin Lowicryl sections labeled with the affinity purified anti-cellubrevin antibody. Micrographs show representative fields of the sinusoidal (*a–e*) or the apical (*f*) regions of hepatocytes. Labeling (10 nm gold) is concentrated mainly in tubules, vesicles, or tubulovesicular structures (*arrowheads*) close to the sinusoidal plasma membrane. In the apical, pericanalicular region, only few small vesicles were labeled (*arrowheads* in *f*). *bc*, bile canaliculus; *sin*, sinusoidal domain. *Bar* is 100 nm.

Ortega *et al.* (Ref. 17)).

Reorganization of Cellubrevin-containing Endocytic Compartment upon IgA Internalization—To assess the possible involvement of cellubrevin containing endocytic structures in the transcytotic route of the hepatic cell, exogenous pIgA (100 μg) was injected into the portal vein and 2.5 and 20 min later livers were removed and immunocytochemical studies were performed (control livers were injected with 0.9% NaCl). Human IgA was efficiently taken up by the liver of normal and estradiol-treated rats; 15 min after intravenous injection, approximately 50% was recovered in the liver (37).

Fig. 5 shows the immunocytochemical localization of cellubrevin in control (0.9% NaCl) and in IgA-injected rats. Rat liver frozen sections were double labeled with anti-cellubrevin antibodies, followed by the secondary fluorescently labeled goat anti-rabbit IgG-FITC and a mouse anti-human IgA followed by a rabbit anti-mouse IgG-Cy 3. Cellubrevin (optical section from confocal microscopy) was mainly concentrated underneath the sinusoidal plasma membrane domain of hepatocytes (Fig. 5*a*). The labeling with anti-mouse human IgA showed little cross-reactivity with the endogenous rat IgA (Fig. 5*b*).

When a pulse of exogenous pIgA (100 μg) was given and livers analyzed 2.5 and 20 min later, it can be observed that, although the subsinusoidal cellubrevin staining remained (*arrowheads*), a subapical cellubrevin labeling emerged in some hepatocytes after 20 min, which co-localized with IgA (Fig. 5*g*, *arrows*; see also overlay *panels c*, *f* and *i*). After 2.5 or 20 min, the exogenous IgA was detected inside the hepatocytes and at the sinusoidal plasma membrane (Fig. 5, *e* and *h*) (in agreement with studies of Hoppe *et al.* (39). *Insets* (in *a*, *g*, *h,* and *i*) show details of the re-organization of cellubrevin-containing structures in the hepatic endocytic compartments after IgA injection.

However, in livers in which dextran-FITC, as a fluid-phase marker (Fig. 6, *a* and *b*), or LDL, a ligand that follows the degradation pathway (*c*, *d*), was injected (for 20 min), the pattern of cellubrevin labeling in the hepatic cell did not change, remaining associated with the subsinusoidal region of hepatocytes. An anti-apoB100 specific antibody was used for the detection of LDL in the intact liver (double labeling was not possible because both antibodies were rabbit polyclonals).

The observation of the immunocytochemical data (Fig. 5) suggested a possible involvement of cellubrevin-containing structures in the transport of IgA from the subsinusoidal region of the hepatocyte to the pericanalicular area onward to transcytosis.

Two experimental approaches provided significant data supporting this idea. First of all, we studied the subcellular distribution of cellubrevin in endosomal fractions from control (NaCl) and from livers previously loaded with pIgA (20 min, 100 μg). Endosomal fractions were prepared and further fractionated, by flotation, in a multistep sucrose gradients as described under "Experimental Procedures." Unloaded samples

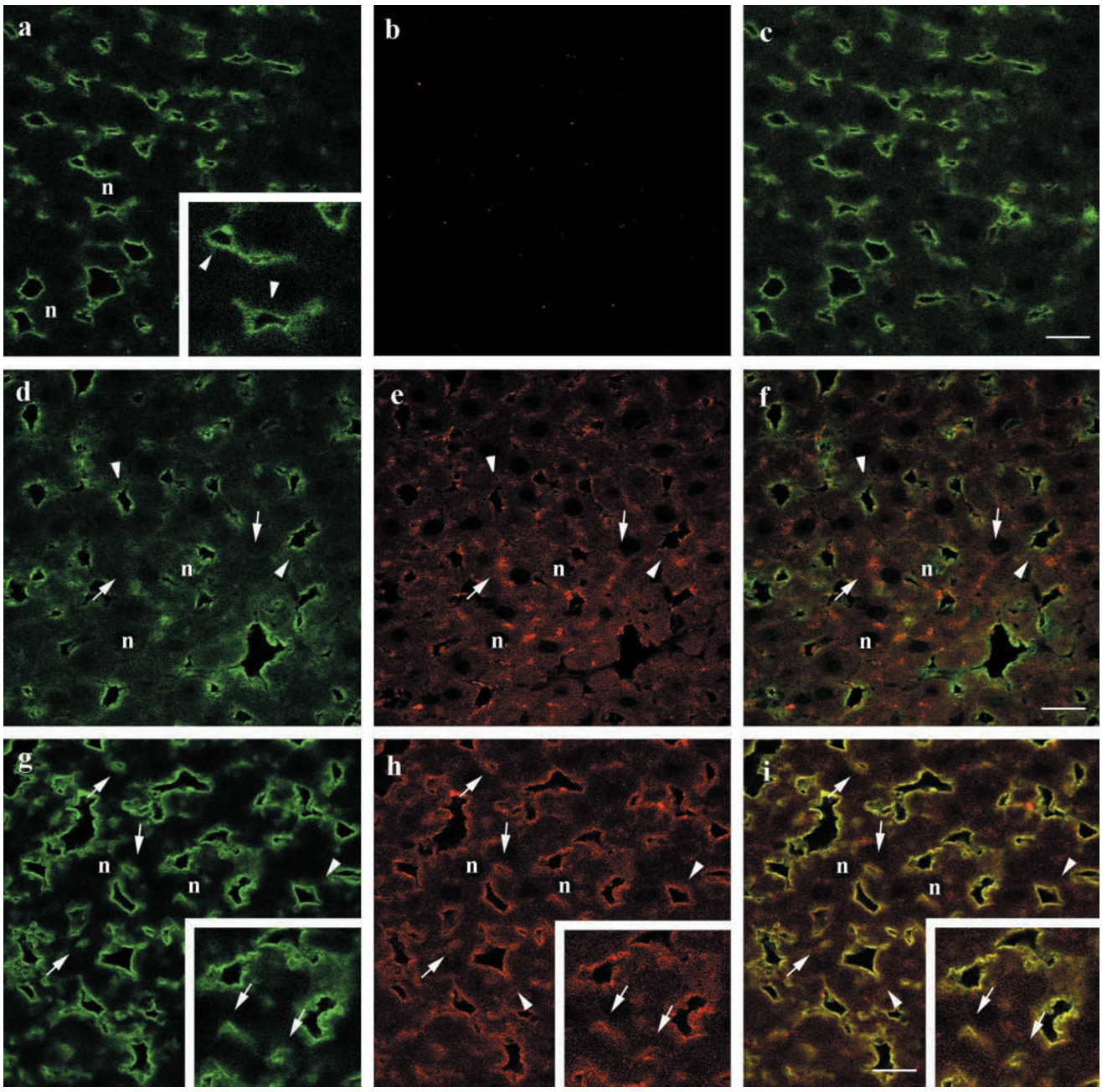

FIG. 5. **Immunocytochemical distribution of cellubrevin and pIgA in rat liver frozen sections.** Human pIgA (100 μg) was intravenously injected in rats, and after 2.5 or 20 min, livers were fixed, removed, and prepared for double immunolabeling with anti-cellubrevin (*a*, *d*, *g*; FITC-labeled) and anti-IgA antibodies (*b*, *e*, *h*; Cy 3-labeled). Cryostat sections (6 μm) were used to study the cellubrevin and IgA distribution in the hepatic tissue. Representative optical sections (1 μm) of fields imaged with a confocal microscopy of control (0.9% NaCl) section where the cellubrevin staining is concentrated in the subsinusoidal region of hepatocytes (*a*); the same field showed that the human anti-mouse IgA did not recognize the endogenous rat IgA (*b*). After 2.5 min of pIgA injection, there was no significant change in the structures containing cellubrevin (*d*). IgA was detected inside but predominantly in the sinusoidal plasma membrane of hepatocytes (*e*). However, after 20 min of IgA some cellubrevin labeling can be observed in the pericanalicular regions (*g*) (*arrows*) although the labeling at the sinusoidal spaces remains (*arrowheads*). Co-localization of the two antibodies indicates that at this time point (20 min) some of cellubrevin endocytic structures contained IgA (*h*). *Panels c*, *f*, and *i* show the merged images. *Insets* show detailed magnified regions for comparison. *n*, nucleus. *Bar* is 10 μm.

were analyzed by Western blotting to find out the distribution of cellubrevin. Fig. 7*a* shows the displacement of the cellubrevin containing endosomal fractions, toward the heavy density range, in both CURL and RRC, after the load with IgA. As a control, the same gradients were analyzed for the distribution of annexin VI; in this case, no change in the patterns of annexin VI distribution along the densities studied in control or in IgA containing fractions could be observed (Fig. 7*b*). A further control included the biochemical analysis of the distribution of endosomal proteins in endocytic fractions with or without the administration of LDL; the results showed no changes in their qualitative or quantitative distribution (data not shown). The distribution of IgA (as control) in the density gradient, after IgA injection, becomes more homogeneous, compared with the control profile (especially in the CURL density range) (Fig. 7*c*).

Second, CURL and RRC fractions, before subfractionation, isolated from control and from livers loaded with pIgA (for 20 min) were used for coimmunoprecipitation experiments, with anti-cellubrevin or anti-pIgR (mouse monoclonal SC-166, which recognizes the cytoplasmic domain of the pIgR), to test whether cellubrevin was associated with pIgR in the endocytic fractions. Interestingly, coimmunoprecipitation takes place in

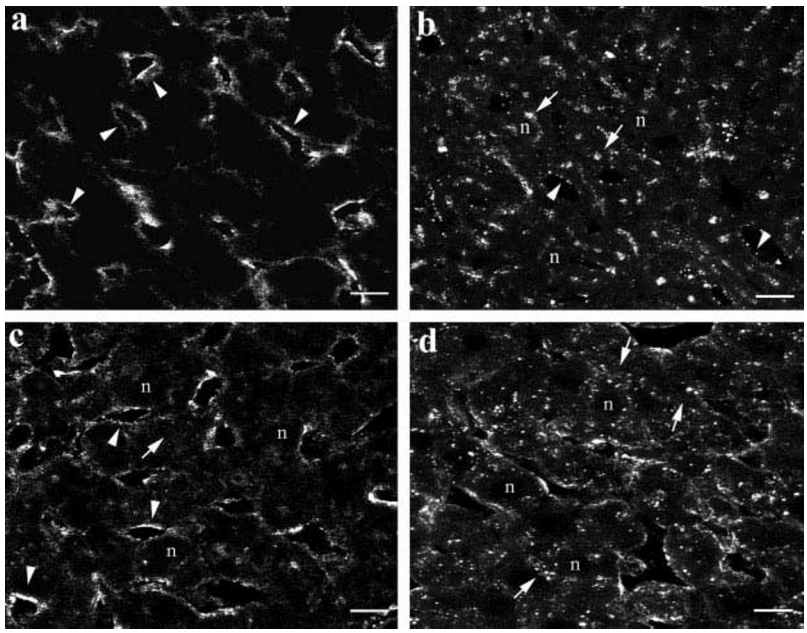

FIG. 6. **Immunofluorescence studies of fluid phase and receptor-mediated endocytosis in rat liver.** Frozen liver sections were used to study the organization and behavior of cellubrevin after the internalization of fluid phase marker, dextran-FITC (M_r 70,000) (*b*) or LDL (*d*), as a ligand that enters via receptor-mediated endocytosis. In *a*, the pattern of cellubrevin is shown after the internalization of dextran-FITC for 20 min; *c* shows the same but after the internalization of LDL (LDL was detected using a rabbit anti-human apoB100 antibody). In all panels, *arrows* point subapical and *arrowheads* subsinusoidal labeled structures. *n*, nucleus; *bar* is 10 μm.

RRC fractions isolated from the livers loaded with IgA (Fig. 7, *d* and *e*).

From these data, we conclude: 1) overloading the transcytotic pathway (with IgA) perturbs the density of those structures in CURL and RRC containing cellubrevin, and 2) cellubrevin and pIgR reciprocally coimmunoprecipitated the other one, only in the RRC fractions isolated from rats loaded with IgA, suggesting that these two proteins must be in the same transcytotic vesicles.

DISCUSSION

According to the SNARE hypothesis, soluble NSF attachment protein (SNAP) receptors on a vesicle membrane (v-SNARE) bind to SNAP receptor proteins on the target membrane (t-SNARE) in the process of vesicle docking. Fusion of the docked vesicle with the target membrane also involves the binding of the soluble proteins α-SNAP and NSF to this SNARE complex, driven by the ATPase activity of NSF. Thus, the v- and t-SNARE families would determine the specificity of vesicular transport. However, a growing body of evidence shows that specificity of the fusion event is a very complex and synchronized process, which also requires other cofactors such as the Rab proteins (Rab5), docking proteins (early-endosomal autoantigen-1, Rabaptin-5), protector proteins (n-Sec1), or "stabilizing" proteins (LMA-1) (for a recent review, see Ref. 40).

Cellubrevin, which belongs to the v-SNARE family, has been implicated in membrane trafficking and in constitutive and regulated secretion. However, although cellubrevin was detected in the liver (5), no attempts to elucidate its subcellular distribution or its involvement in the secretory or endocytic pathways in the hepatocyte have been reported.

Hepatocytes display two independent constitutive secretory pathways: one to the blood, through the basolateral plasma membrane (*e.g.* lipoproteins, albumin, or fibronectin) and a second into the bile through the apical, canalicular, plasma membrane (*e.g.* bile acids). Transcytosis, a major intracellular transport pathway unique to polarized epithelial cells, is an additional constitutive secretory route. Very few proteins have been identified as being involved in its regulation in the hepatocyte (41–43) or in MDCK cells (44–48). Interestingly, calmodulin and several calmodulin-binding proteins in the cortical cytoskeleton may be crucial for the regulation of the first and last steps of transcytosis (for example: myosin I, gelsolin, α-actinin, spectrin, or adducin) (33, 35).

While cellubrevin has been related to early recycling events in non-polarized cells (6, 49), its function in polarized epithelial cells is unknown. Several studies have shown the distribution of different SNAREs in polarized cells (7, 8, 50, 51); cellubrevin was detected in intracellular organelles localized both in the lateral and in the apical domains of CaCo-2 cell line (8).

Recently, a study in rat liver showed the distribution of different endogenous syntaxins (t-SNARES) in the hepatocyte plasma membrane. Interestingly, syntaxin 2 and 3 were shown to be enriched in the apical plasma membrane, whereas syntaxin 4 was mainly expressed in the sinusoidal plasma membrane (52). A significant amount of syntaxin 3 was also detected in subcellular fractions containing transport vesicles. Syntaxins 2 and 3 were found enriched in the RRC and in CURL endosomal fractions from rat liver (53).

Whether syntaxins confer specificity to the targeting event remains to be determined, but the predominant location of those syntaxins in the canalicular plasma membrane might be a signal for a major docking of the corresponding v-SNARE. If cellubrevin were involved in the apical transcytosis in the hepatocyte, then a so far unidentified t-SNARE would be binding partner. Since syntaxins 2 and 3 are located in the bile canalicular plasma membrane, they are good candidates for cellubrevin interaction. Interestingly, in CaCo-2 cells, it has been demonstrated that syntaxin 3 and SNAP23 form apical SNARE complexes, which provides the first evidence for the involvement of cellubrevin and a new v-SNARE, TI-VAMP (tetanus neurotoxin-insensitive VAMP), in apical SNARE complex formation (8). In these studies, the NEM treatment of CaCo-2 cells increased the recovery of cellubrevin and SNAP-23 associated with syntaxin 3; these authors reach the conclusion that cellubrevin- and TI-VAMP-containing vesicles dock at the apical plasma membrane through the NEM-dependent formation of SNARE complexes, which include SNAP23 and syntaxin 3.

The role of syntaxins in transcytosis was examined in MDCK cells (54); transcytosis to the apical surface has been shown to be dependent, at least in part, on NSF and a substrate that is cleaved by botulinum E toxin, most likely a homologue of SNAP-25. Therefore ,apical transcytosis may depend on a syntaxin (55). However, considering the published localization of

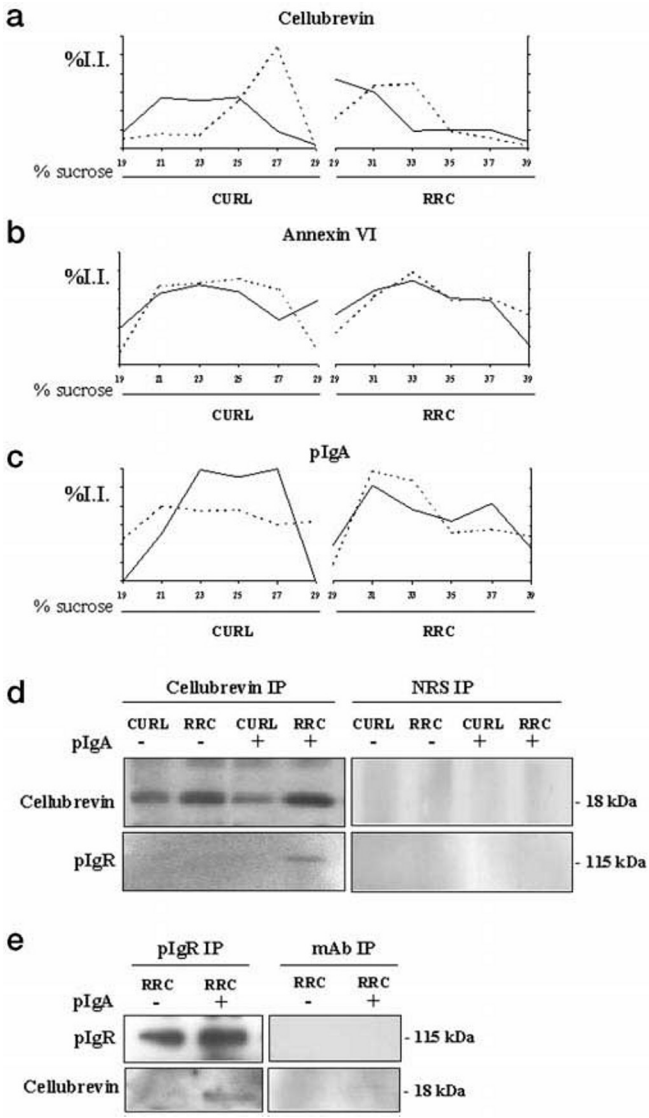

FIG. 7. **Subcellular distribution and co-immunoprecipitation of cellubrevin in IgA-loaded endocytic fractions.** Subcellular distribution of cellubrevin (*a*), annexin VI (*b*), and IgA (*c*) in control endocytic fractions and after exogenous IgA (100 μg) administration. Isolated endosomes (CURL and RRC) from control or the same fractions from rats injected with IgA (for 20 min) were loaded at the bottom of a multistep sucrose gradients (19–29%, CURL or 29–39%, for RRC). Tubes were centrifuged for 170 min at 28,000 rpm. After gradient fractionation, samples were pelleted and resuspended in 0.9% NaCl, electrophoresed, and transferred electrophoretically to Immobilon-P membranes. Cellubrevin, annexin VI, and IgA were detected by Western blotting. Bands were densitometrically quantified, and the intensity of each band was expressed as a percentage of the total intensity. *I.I.*, integrated intensity. *Continuous line*, control endosomes; *dashed line*, endosomes from livers loaded with IgA. In *d* and *e*, pIgR and cellubrevin coimmunoprecipitate. In *d*, immunoprecipitation (*IP*) of cellubrevin followed by immunoblot using pIgR-specific antibodies (mouse monoclonal SC-166); cellubrevin was immunoprecipitated in CURL and RRC control and from pIgA-containing fractions. Coimmunoprecipitation of pIgR was detected in RRC isolated fraction from rats injected with pIgA. In *e*, immunoprecipitation of pIgR followed by immunoblot using anti-cellubrevin-specific antibodies. pIgR was immunoprecipitated in RRC fractions with or without pIgA, whereas coimmunoprecipitation of cellubrevin was detected in RRC fraction of pIgA-treated rats. Immunoprecipitation using a normal rabbit serum (*NRS*) or a monoclonal non-related antibody (*mAb*) were used as controls. In all experiments, rats were treated with estradiol and loaded with LDL.

the plasma membrane syntaxins in MDCK cells (7) and the finding that synaptobrevin/VAMP-2 binds *in vitro* to the basolateral syntaxin 4 but not to the apical syntaxins 2 or 3 (56, 57), it seems only natural that apical membrane fusion should not involve synaptobrevin/VAMP-2 and therefore is toxin-insensitive (54).

In this study, for the first time, we show that in hepatocytes, cellubrevin is almost restricted to tubulovesicular endocytic structures in the subsinusoidal region. In isolated endosomes from rat liver, it was enriched in the early/sorting and in the "recycling" endosomes (58). The finding that cellubrevin was subsequently enriched in a subpopulation of early endosomes together with pIgA suggests that it may be committed to the transport, from these early endosomes, into the transcytotic pathway. This was supported in those experiments in which the transcytotic pathway was overloaded with IgA; first, it causes the formation of cellubrevin structures with a higher density than those from the control, and, second, the reciprocal coimmunoprecipitation of cellubrevin and pIgR from RRC suggest that cellubrevin and pIgR are in the same vesicle. Thus, cellubrevin becomes the third molecule with specific physical association with the pIgR (calmodulin was the first (Ref. 33), and $p62^{yes}$ the second (Ref. 26)).

Morphological approaches and the subcellular dissection of early endocytic compartment of rat liver revealed: (i) that cellubrevin may be a marker for the subsinusoidal endosomes and (ii) the fact that cellubrevin-containing structures in the hepatocyte are transported together with pIgR-IgA from these early/sorting endosomes (subsinusoidal domain), along the transcytotic pathway, to the subapical endocytic compartment is consistent with the recent view of the involvement of SNAREs in transcytosis (59).

Finally, the presence of Raf-1 in the same endocytic subcompartment as cellubrevin suggests the functional complexity of the subsinusoidal endocytic compartment of the hepatocyte. Work in progress is focused on the molecular characterization of the cellubrevin-pIgR interaction and to further understand the involvement of cellubrevin in the transcytotic route.

Acknowledgments—We are grateful to Serveis Científic i Tècnics Universitat de Barcelona for the electron microscopy facilities and to Anna Bosch for excellent assistance in the confocal microscopy.

REFERENCES

1. Mellman, I. (1996) *Annu. Rev. Cell Dev. Biol.* **12,** 575–625
2. Stoorvogel, W., Strous, G. J., Geuze, H. J., Oorschot, V. & Schwartz, A. L. (1991) *Cell* **65,** 417–427
3. Gruenberg, J., Griffiths, G. & Howell, K. E. (1989) *J. Cell Biol.* **108,** 1301–1316
4. Gibson, A., Futter, C. E., Maxwell, S., Allchin, E. H., Shipman, M., Kraehenbulh, J.-P., Domingo, D., Odorizzi, G., Trowbridge, I. S. & Hopkins, C. R. (1998) *J. Cell Biol.* **143,** 81–94
5. McMahon, H. T., Ushkaryov, Y. A., Edelman, L., Link, E., Binz, T., Niemann, H., Jahn, R. & Südhof, T. C. (1993) *Nature* **364,** 346–349
6. Daro, E., van der Sluijs, P., Galli, T. & Mellman, I. (1996) *Proc. Natl. Acad. Sci. U. S. A.* **93,** 9559–9564
7. Low, S. H., Chapin, S. J., Weimbs, T., Kömüves, L. G., Bennett, M. K. & Mostov, K. E. (1996) *Mol. Biol. Cell* **7,** 2007–2018
8. Galli, T., Zahaoui, A., Vaidyanathan, V. V., Raposo, G., Tian, J. M., Karin, M., Niemann, H. & Louvard, D. (1998) *Mol. Biol. Cell* **9,** 1437–1448
9. Kipp, H., Sai, Y. & Arias, I. M. (1998) *Mol. Biol. Cell* **9,** 209a
10. Ali, N. & Evans, W. H. (1990) *Biochem. J.* **271,** 193–199
11. van Ijzendoorn, S. C. D. & Hoekstra, D. (1998) *J. Cell Biol.* **142,** 683–696
12. George, C. H., Kendall, J. M. & Evans, W. H. (1999) *J. Biol. Chem.* **274,** 8678–8685
13. Barr, V. A. & Hubbard, A. L. (1993) *Gastroenterology* **105,** 554–571
14. Barroso, M. & Sztul, E. S. (1994) *J. Cell Biol.* **124,** 83–100
15. Enrich, C. & Evans, W. H. (1989) *Eur. J. Cell Biol.* **48,** 344–352
16. Tuma, P. L., Finnegan, C. M. & Hubbard, A. L. (1999) *J. Cell Biol.* **145,** 1089–1102
17. Ortega, D., Pol, A., Biermer, M., Jäckle, S. & Enrich, C. (1998) *J. Cell Sci.* **111,** 261–269
18. 16 Pol, A., Calvo, M. & Enrich, C. (1998) *FEBS Lett.* **441,** 34–38
19. Havel, R. J., Eder, H. A. & Bragdon, J. H. (1955) *J. Clin. Invest.* **34,** 1345–1353
20. Majó, G., Aguado, F., Blasi, J. & Marsal, J. (1998) *Life Sci.* **62,** 607–616
21. Chao, Y. S., Windler, E. E, Chen, G. C. & Havel, R. J. (1979) *J. Biol. Chem.* **254,** 11360–11366
22. Belcher, J. D., Hamilton, R. L., Brady, S. E., Hornick, C. A., Jäckle, S., Schneider, W. J. & Havel, R. J. (1987) *Proc. Natl. Acad. Sci. U. S. A.* **84,** 6785–6789
23. Jäckle, S., Runquist, E. A., Miranda-Brady, S. & Havel, R. J. (1991) *J. Biol. Chem.* **266,** 1396–1402

24. Neville, D. M., Jr. (1960) *J. Biophys. Biochem. Cytol.* **8,** 413–422
25. Laemmli, U. K. (1970) *Nature* **227,** 680–685
26. Luton, F., Vergés, M., Vaerman, J.-P., Sudol, M. & Mostov, K. E. (1999) *Mol. Cell* **4,** 627–632
27. Bradford, M. M. (1976) *Anal. Biochem.* **72,** 248–254
28. Bissell, D. M., Hammker, L. E. & Meyer, U. A. (1973) *J. Cell Biol.* **59,** 722–734
29. Jäckle, S., Brady, S. E. & Havel, R. J. (1989) *Proc. Natl. Acad. Sci. U. S. A.* **86,** 1880–1884
30. Jäckle, S., Runquist, E., Brady, S., Hamilton, R. L. & Havel, R. J. (1991) *J. Lipid Res.* **32**, 485–498
31. Jäckle, S., Rinninger, F., Lorenzen, T., Greten, H. & Windler, E. (1993) *Hepatology* **17,** 455–465
32. Jäckle, S., Beisiegel, U., Rinninger, F., Buck, F., Grigoleit, A., Block, A., Groger, L., Greten, H. & Windler, E. (1994) *J. Biol. Chem.* **269,** 1026–1032
33. Chapin, S. J., Enrich, C., Aroeti, B., Havel, R. J. & Mostov, K. E. (1996) *J. Biol. Chem.* **271,** 1336–1342
34. Pol, A., Ortega, D. & Enrich, C. (1997) *Biochem J.* **323,** 435–443
35. Pol, A., Ortega, D. & Enrich, C. (1997) *Biochem J.* **327,** 741–746
36. Pol, A. & Enrich, C. (1997) *Electrophoresis* **18,** 2548–2557
37. Enrich, C., Jäckle, S. & Havel, R. J. (1996) *Hepatology* **24,** 226–232
38. Pol, A., Calvo, M., Lu. A. & Enrich, C. (1999) *Hepatology* **29,** 1848–1857
39. Hoppe, C. A., Connolly, T. P. & Hubbard, A. L. (1985) *J. Cell Biol.* **101,** 2113–2123
40. Pfeffer, S. R. (1999) *Nat. Cell Biol.* **1,** 17–22
41. Sztul, E., Kaplin, A., Saucan, L. & Palade, G. E. (1991) *Cell* **64,** 81–89
42. Quintart, J., Baudhuin, P. & Courtoy, P. J. (1989) *Eur. J. Biochem.* **184,** 567–574
43. Jin, M., Saucan, L., Farquhar, M. G. & Palade, G. E. (1996) *J. Biol. Chem.* **271,** 30105–30113
44. Lütcke, A., Jansson, S., Parton, R. G., Chavrier, Ph., Valencia, A., Huber, L. A., Lehtonen, E. & Zerial, M. (1993) *J. Cell Biol.* **121,** 553–564
45. Hunziker, W. & Peters, P. J. (1998) *J. Biol. Chem.* **273,** 15734–15741
46. Hunziker, W. (1994) *J. Biol. Chem.* **269,** 29003–29009
47. Llorente, A., Garred, Ø., Holm, P. K., Eker, P., Jacobsen, J., van Deurs, B. & Sandvig, K. (1996) *Exp. Cell Res.* **227,** 298–308
48. Apodaca, G., Enrich, C. & Mostov, K. E. (1994) *J. Biol. Chem.* **269,** 19005–19013
49. Calakos, N., Bennett, M. K., Peterson, K. E. & Scheller, R. H. (1994) *Science* **263,** 1146–1149
50. Pevsner, J., Hsu, S. C., Braun, J. E., Calakos, N., Ting, A. E., Bennett, M. K. & Scheller, R. H. (1994) *Neuron* **13,** 353–361
51. Teter, K., Chandy, G., Quiñones, B., Pereyra, K., Machen, T. & Moore, H.-P. H. (1998) *J. Biol. Chem.* **273,** 19625–19633
52. Fujita, H., Tuma, P. L., Finnegan, C. M., Locco, L. & Hubbard, A. L. (1998) *Biochem. J.* **329,** 527–538
53. Vergés, M., Havel, R. J. & Mostov, K. E. (1999) *Proc. Natl. Acad. Sci. U. S. A.* **96,** 10146–10151
54. Low, S. H., Chapin, S. J., Wimmer, C., Whiteheart, S. W., Kömüves, L. G., Mostov, K. E. & Weimbs, T. (1998) *J. Cell Biol.* **141,** 1503–1513
55. Apodaca, G., Cardone, M. H., Whiteheart, S. W., DasGupta, B. R. & Mostov, K. E. (1996) *EMBO J.* **15,** 1471–1481
56. Regazzi, R., Wollheim, C. B., Lang, J., Theler, J.-M., Rossetto, O., Montecucco, C., Sadoul, K., Weller, U., Palmer, M. & Thorens, B. (1993) *EMBO J.* **14,** 2723–2730
57. Leung, S.-M., Chen, D., DasGupta, B. R., Whiteheart, S. W. & Apodaca, G. (1998) *J. Biol. Chem.* **273,** 17732–17741
58. Enrich, C., Pol, A., Calvo, M., Pons, M. & Jäckle, S. (1999) *Hepatology* **30,** 1115–1120
59. Yeaman, C., Grindstaff, K. K. & Nelson, J. (1999) *Physiol. Rev.* **79,** 73–98